Polymer Bulletin 37, 103–110 (1996)

Polymer Bulletin

Effect of temperatures on the mechanical and morphological properties of polyphenylene sulfide composites

Hern-Jin Park [1], **Byoung Chul Chun** [2,*]

[1] Advanced Materials Team, SKI Corporate R&D Center, Kyonggi-do, Korea
[2] Department of Polymer Engineering, College of Engineering, University of Suwon, Hwasung-gun, Kyonggi-do, Korea

Received: 2 February 1996/Revised version: 8 April 1996/Accepted: 11 April 1996

Summary

Mechanical properties and corresponding microstructures of polyphenylene sulfide(PPS)/glass fiber composites were investigated according to the glass fiber content and testing temperature change. Tensile test results showed that maximum stress and elastic modulus increased markedly with increasing glass fiber content at below the glass transition temperature(T_g) of PPS matrix. Notched Izod impact strength showed a maximum value at the glass fiber content of 40 wt% regardless of testing temperatures. Scanning electron microscope (SEM) observation of tensile and impact fractured specimens showed that, at the same testing temperature condition, the fracture surface became more rugged as the glass fiber content increased. Polarized optical microscope(POM) observation showed the crack tip bifurcation at the glass fiber surface in tensile fractured specimens, whereas glass fiber breakdown in impact fractured specimens at higher glass fiber content.

Introduction

Polyphenylene sulfide(PPS) is an engineering plastic polymerized by the reaction of p-dichlorobenzene and sodium sulfide in a polar solvent. It was first commercialized in 1973 by Philips Petroleum Company as a trade name of Ryton, and since then its use was expanded into electronic, electrical, automotive and mechanical applications (1, 2). PPS can be made into glass fiber reinforced composites and these composites are lighter and stronger than comparable metals and their compositions can be easily changed according to the applications. PPS has the glass transition temperature of 80-90°C and melting temperature of about 290°C, and has high temperature resistance, chemical resistance, precision moldability, dimensional stability, electrical properties, flame resistance, stiffness, creep resistance, affinity for a variety of fillers and reinforcing agents. Recycled PPS can also be safely used without much deterioration of properties, thus this make PPS as a good candidate material for reducing the environmental damage.

Shingankuli et al. studied the thermal and crystallization behavior of PPS and polyethylene terephthalate blends, and found that the degree of crystallinity of PPS was reduced as the PET content increased (3). Desio and Rebenfeld studied the effect of fibers on the crystallization of PPS. They found that aramid and carbon fiber decreased the crystallization half-time, whereas the glass fiber affected the crystallization half-time only at the higher crystallization temperatures (4). Budgell and Day studied the crystallization behavior of PPS, and found that thermal history of the sample played an important role in determining the crystallization kinetics (5). Besides these investigations, there has been research on the crystallization and thermal behavior of PPS composites and blends in recent years (6-13).

Meanwhile, Fagerburg et al. studied the rheological properties of PPS, and found that the melt viscosity increased during the rheological testing due to the chain branching and extrusion effect (14). Caramaro et al. studied the morphology and mechanical properties of PPS/carbon fiber composites, and found that mechanical properties could be optimized by controlling the molding conditions and the matrix morphology (15). Chung and Cebe studied the morphology of PPS single crystals to investigate the morphological changes dependent upon the seeding and crystallization conditions (16). Heino and Seppala studied the structure-property relationship of PPS/thermotropic liquid crystalline polymer (LCP) blend, and found

* Corresponding author

that LCP acted as a significant reinforcement for PPS matrix (17).

From the above literature survey, majority of research was done regarding the thermal and crystallization behavior of PPS composites or blends. Few research was conducted on the mechanical properties and morphology of PPS composites. In this investigation, systematic studies of the effect of glass fiber content and testing temperature on the mechanical and morphological behavior of PPS composites are conducted.

Experimental

1. Sample preparation

PPS used in this investigation was a commercial grade resin(SKI, Suntra S-500, M_w = 30,000 g/mol). E-glass fiber was supplied by Lucky Co.(length : 3 mm, diameter : 13 μm, density : 2.7 g/cm^3) and was surface treated with silane coupling agent(Dow Corning, 3-(N-styrylmethyl-2-amino-ethylamino) propyltrimethoxy silane hydrochrolide). Compounding was done using the Toshiba compounder(twin screw extruder, co-rotating intermeshing type, ϕ= 35 mm), and temperature was maintained at 315-320°C, and screw rpm was 350. Mechanical specimens were manufactured using the injection molder(Engel, 75 ton). Table 1 shows the compositions and thermal properties of PPS composites used in this investigation.

Table 1. Compositions and thermal properties of PPS/glass fiber composites prepared in this investigation.

PPS (wt%)	100	80	60	50
Glass fiber (wt%)	0	20	40	50
Glass transition temperature (℃)	89.6	90.4	90.1	90.1
Melting temperature (℃)	282.4	282.9	282.0	280.5
Degree of crystallinity (%)	49.8	50.3	49.8	51.8
Code. No.	PPS-0	PPS-20	PPS-40	PPS-50

2. Mechanical testing

Tensile properties of PPS composites were measured using universal testing machine(Lloyd Instruments, LR 50K). ASTM D-638 size specimens were tested with a constant crosshead speed of 50 mm/min, gauge length of 50 mm, and laser extensometer was used. All specimens were tested at 25, 75, 125 and 175°C using the thermal cabinet, and at least five specimens of each composition were tested, and the average value was used to plot the data. Notched Izod impact strength was measured using the impact tester(Testing Machine Inc. Model 43-02, Pendulum 75 kgcm, Izod type) and all specimens were also tested at the above four different temperatures. Impact specimens were manufactured to the ASTM D-256 specification, and at least 10 specimens were tested and the average value was used for the data plot except the maximum and minimum values.

3. Morphological analysis

Tensile and impact fractured specimens were coated with gold using ion sputtering machine, and their fracture morphologies were investigated using the scanning electron microscope(SEM, Akashi ISI-DS 130). The operating voltage was 10kV. For the subsurface microstructure analysis, the area containing the fracture surface was cut using the jeweller's saw. This cutout was placed on the glass slide using double sided tape and held in the petrographic slide holder. One surface was ground using silicon carbide emery paper(240, 320, 400, 600 grit) and polished with alumina paste(N, F type) using grinding

machine(Buehler UK Ltd., Metaserv 2000). The polished surface was then placed on the glass slide using Devcon 5-minutes epoxy. This procedure was repeated and final polished sample was observed using polarized optical microscope(POM, Nikon Optiphot 2-POL) to investigate the glass fiber and crack distribution. Also the glass fiber diameter of tensile and impact fractured specimens were quantitatively analyzed using the image analyzer(Media Cybernetics, Image-Pro plus for window 1.2)

Results and discussion

Tensile testing and morphology analysis

Fig. 1 and 2 show the maximum stress and elastic modulus of PPS composites at various testing temperatures. As can be seen in these figures, maximum stress and elastic modulus increased rapidly at the testing temperatures of 25 and 75°C. However, at above these temperatures, this increase effect was diminished. At the temperature above the T_g of PPS, PPS matrix becomes rubbery and ductile. At this condition, fracture can occur in the matrix or matrix-glass fiber interface rather than the glass fiber itself and this account for the fact that the maximum stress and elastic modulus did not increase dramatically at the higher testing temperatures.

Fig. 3 shows the strain at break of PPS composites. At the testing temperatures of 25 and 75°C, strain at break was less than 2.5%. At this temperature range, glass fiber content change did not affect the percent strain at break. However, above the T_g of PPS matrix, the situation becomes quite different. At 125 and 175°C, PPS-0 did not break up to 100% strain, and as the glass fiber content becomes more than 20wt%, the strain at break finally started to decrease. However, even at the glass fiber content of 50wt%, the percent strain at break of PPS-50 tested at 125 and 175°C was twice higher than PPS-50 tested at 25 and 75°C. This is probably due to the fact that at the temperature above T_g of PPS, rubbery PPS matrix can absorb a larger amount of strain without the fracture and this result can be understood by observing the tensile fractured surfaces.

Fig. 4 (a) and (b) show the tensile fractured surfaces of PPS-20 tested at 25 and 175°C, and Fig. 4 (c) shows the tensile fractured surface of PPS-40 tested at 175°C. As can be seen in Fig. 4(a), the surface of pulled out glass fiber is very clear due to the poor interfacial bonding between the PPS matrix and glass fiber. Fig. 4 (b) shows the glass fiber covered with PPS resin. Thus, testing temperature might affect the interfacial bonding between the glass fiber and PPS resin. As can be seen in Fig. 4 (b) and (c), as the glass fiber content increased at the same testing temperature, more plastic deformation occurred and resulted in a more PPS resin wetting the glass fiber surface. This led to a maximum stress and elastic modulus increase, however, decrease in percent strain at break due to the glass-rubber transition with respect to T_g of PPS matrix.

Fig. 5 shows the results of work done which represent the toughness of material. As can be seen in this figure, there is a large difference in behavior with respect to T_g of PPS. As the glass fiber content increased at 25 and 75°C, toughness increased, however, at 125 and 175°C, toughness decreased. Especially, at the glass fiber content of 20wt%, toughness values were quite different depending on the testing temperatures. This results indicate the importance of interfacial bonding between PPS matrix and glass fiber. Depending on the testing temperature, the interfacial bonding played an important role in determining the total strain as shown in Fig. 3, and this strain at break discrepancy resulted in a large difference in toughness values. According to the image analyses results shown in Table 2, the original glass fiber diameter was 13μm(Fig. 4(a)), whereas, in Fig. 4 (b) and (c) the diameter measured considering the tilt angle between the SE detector and sample surface was about 16μm. This indicates that at higher temperatures, PPS matrix is in a rubbery state and absorb a larger amount of strain before the fracture. And as the glass fiber content increases, the relative amount of PPS matrix becomes smaller and results in a strain at break decrease. However, at 25 and 75°C, PPS matrix is in a glassy state, and at this state, glass fiber content does not play a critical role in determining the strain at break as in rubbery state, and results in an almost

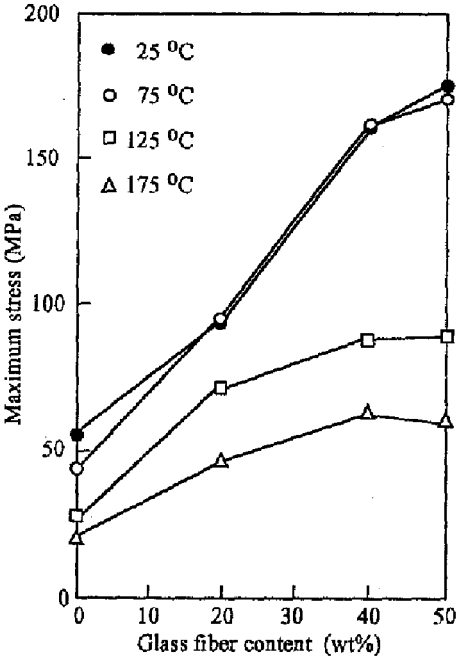

Fig. 1 Maximum stress vs. glass fiber content of PPS/glass fiber composites at various testing temperaturetures.

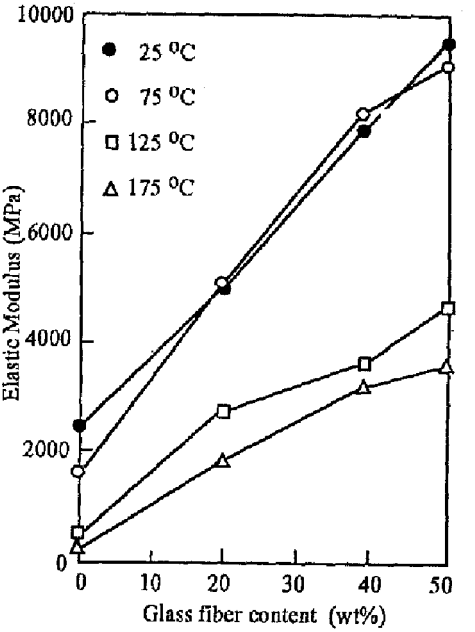

Fig. 2 Elastic modulus vs. glass fiber content of PPS/glass fiber composites at various testing temperatures.

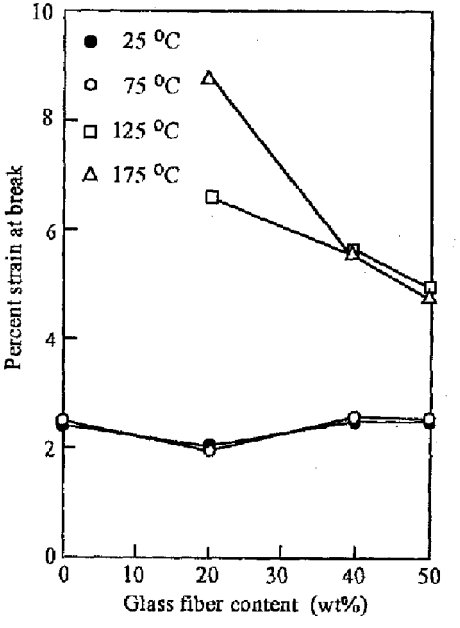

Fig. 3 Percent strain at break vs. glass fiber content of PPS/glass fiber composites at various testing temperatures.

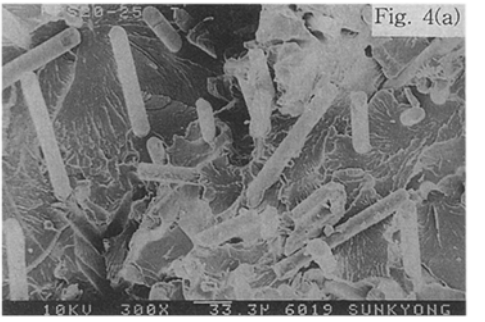

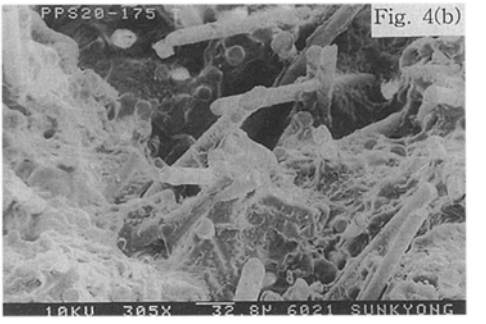

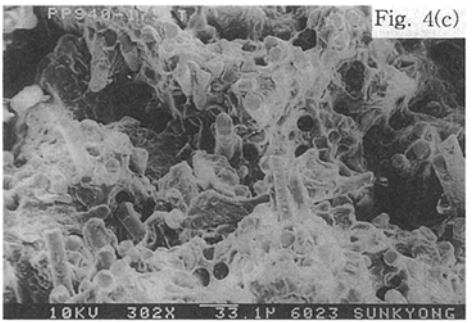

Fig. 4 SEM micrographs of tensile fractured surface of PPS/glass fiber composites at various testing temperatures.
(a) PPS-20(25°C) (b) PPS-20(175°C)
(c) PPS-40(175°C)

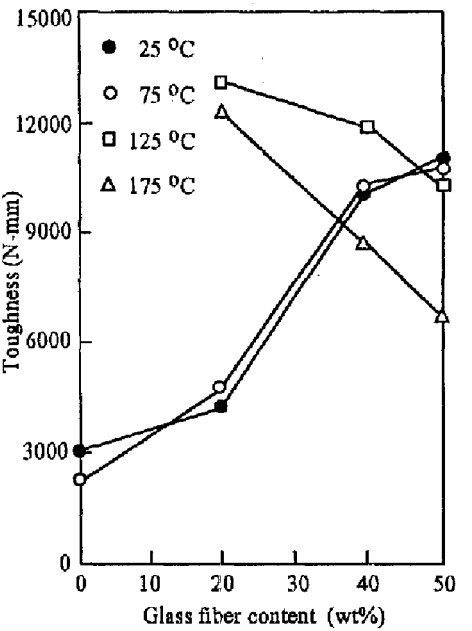

Fig. 5 Toughness vs. glass fiber content of PPS/glass fiber composites at various testing temperatures.

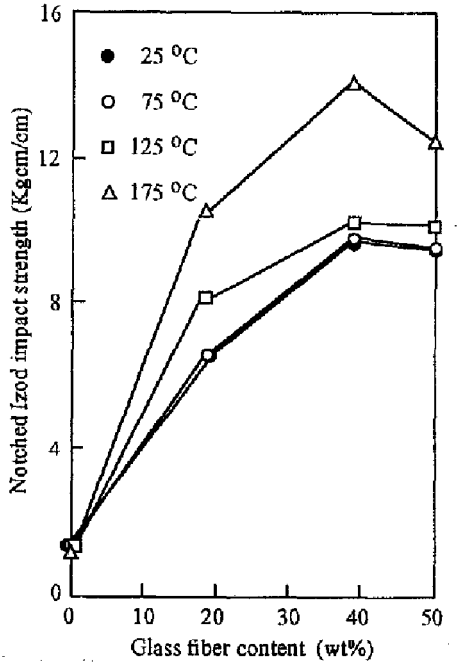

Fig. 6 Notched Izod impact strength vs. glass fiber content of PPS/glass fiber composites at various testing temperatures.

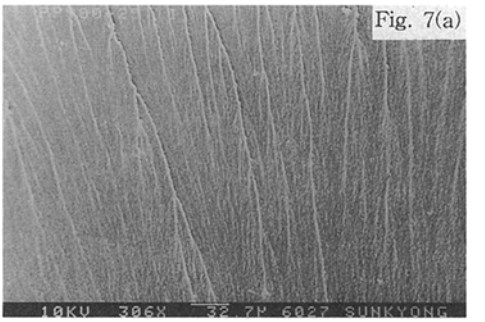

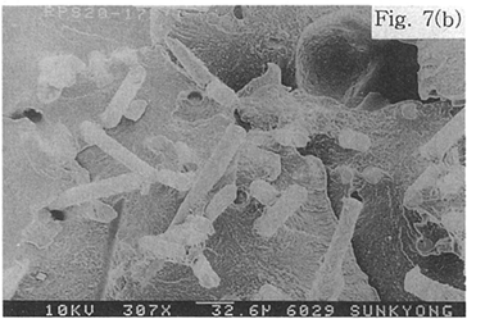

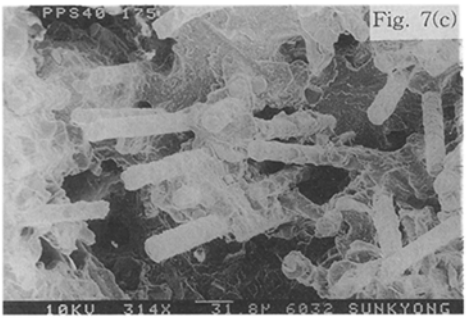

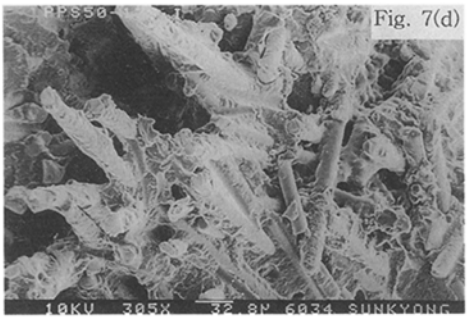

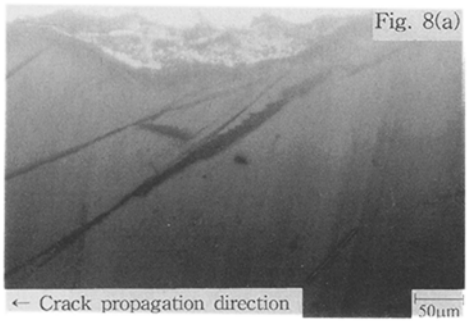

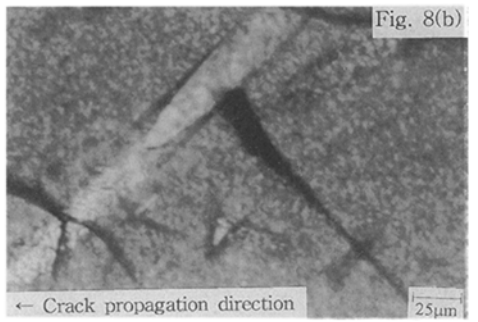

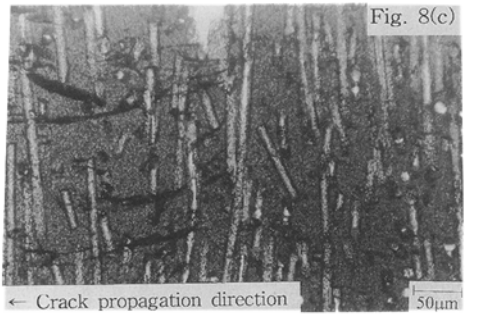

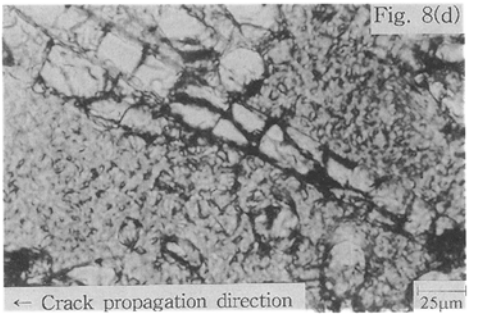

Fig. 7 SEM micrographs of impact fractured surface of PPS/glass fiber composites tested at 175°C.
(a) PPS-0
(b) PPS-20
(c) PPS-40
(d) PPS-50

Fig. 8 Optical micrographs with crossed polarizers showing the subsurface microstructure of PPS/glass fiber composites at various testing temperatures.
(a) PPS-0 (tensile fractured at 25°C, magnification: x 200)
(b) PPS-20 (tensile fractured at 25°C, magnification: x 400)
(c) PPS-20 (impcat fractured at 25°C, magnification: x 200)
(d) PPS-40 (impact fractured at 125°C, magnification: x 400)

constant strain at break.

Table 2. Average fiber stem diameters measured by image analyzer from SEM micrographs of debonded glass fiber in tensile and notched Izod impact fractured specimens.

Testing temperature (℃)	25			175		
Code No.	PPS-20	PPS-40	PPS-50	PPS-20	PPS-40	PPS-50
Tensile fractured specimem (μm)	13.7	13.7	13.3	16.2	16.2	16.7
Impact fractured specimem (μm)	16.2	16.0	16.1	19.7	20.3	20.2

Impact testing and morphology analysis

Material impact strength can be defined as the energy absorbed per unit area of the broken cross-section by the sudden blow and this is represented by the sum of material deformation energy and fracture propagation energy. Fracture in a composite material is generally devided into three modes, fracture of matrix, fracture of fiber, and fracture of matrix/fiber interface, and in impact testing, fracture generally occurs in a mixed modes. This means that the composites properties are dependent upon the interfacial properties as well as matrix and reinforcement.

Fig. 6 shows the notched Izod impact strength of PPS composites. PPS-0 showed little notched Izod impact strength difference between testing temperatures. As the glass fiber content increased, the notched Izod impact strength increased and at the glass fiber content of 40wt%, it had the maximum values regardless of testing temperaure. Especially at the testing temperature of 25 and 75°C, the notched Izod impact strength has an almost same values, and this indicates that the temperature below the T_g of PPS matrix, temperature does not play an impartant role in increasing the impact strength. However, at the temperature higher than T_g, notched Izod impact strength increased further as the testing temperature increased. This is due to the fact that at the temperature above T_g, PPS matrix is in a rubbery state and it can absorb a larger amount of impact energy before it transmit this energy to glass fiber reinforcement.

Fig. 7 (a) - (d) show the SEM micrographs of impact fractured surfaces at the testing temperature of 175°C as the glass fiber content increases. Fig. 7 (a) shows the river patterns generally observed in a brittle non-reinforced PPS. Fig. 7 (b) shows a glass fiber pull-out with a plastic deformation of PPS matrix. Compared to the tensile fractured PPS-20 at 175°C, the fiber diameter of impact fractured specimens is 19.7 μm vs. 16.2 μm of tensile fractured specimens. Fig. 7 (b) - (d) shows the more severe matrix plastic deformation and glass fiber wettings as the glass fiber content increases. By comparing Fig. 7 (c) and (d), Fig. 7 (d) shows fiber bundled together as compared to Fig. 7 (c) which shows individual fiber pull-out with PPS matrix wetting the glass fiber surface. Thus, this fiber bundle and resultant decrease in fiber to fiber distance probably account for a decrease of impact strength due to the rapid and direct transmission of impact energy.

Subsurface microstructure analysis

Fig. 8 (a) - (d) show the subsurface microstructure of PPS composites observed through polarized opital microscope(POM) with crossed polarizers. Fig. 8 (a) shows the subsurface microstructure of tensile fractured PPS-0 tested at 25°C near the fracture surface. As can be seen in this figure, there are fewer but longer cracks in the vicinity of main fracture surface. Fig. 8 (b) shows the subsurface microstructure of tensile fractured PPS-20 tested at 25°C in the central region just below the main fracture surface. It shows many cracks around the glass fiber and indicates there are numerous cracks occurred throughout the sample area. It also shows that the crack propagation is bifurcated at the glass fiber and in some cases crack can

initiate from the glass fiber surface. Fig. 8 (c) shows the subsurface microstructure of impact fractured PPS-40 tested at 25°C. This figure shows many short cracks parallel to the main fracture surface direction and crack propagation is also interrupted or bifurcated by the presence of glass fiber. Fig 8 (d) shows the subsurface microstructure of impact fractured PPS-50 tested at 125°C. It shows the glass fiber breakdown in the vicinity of main fracture surface. This type of glass fiber breakdown is observed in the impact fractured specimens at higher glass fiber content and it indicates that glass fiber can absorb a large amount of impact energy and results in a higher impact strength at higher glass fiber content.

Conclusions

Mechanical properties and morphology of PPS/glass fiber composites were investigated and following conclusions can be made.

1. Maximum stress and elastic modulus showed an increase with increasing glass fiber content and decreasing testing temperature. Percent strain at break showed a decrease with increasing glass fiber content tested at 125 and 175°C, however, remained almost the same at 25 and 75°C.
2. Notched Izod impact strength showed an increase with increasing glass fiber content and temperature, however, had a maximum value at the glass fiber content of 40wt% regardless of testing temperature.
3. SEM observation showed that at the same testing temperature, tensile and impact fractured surface became more rugged as the glass fiber content increased. At the same glass fiber content, more matrix plastic deformation and glass fiber wetting was found as the testing temperature increased. POM observation showed that the short and numerous cracks dominated along the entire impact fractured specimens and glass fiber breakdown at the higher glass fiber content was found, whereas, in tensile fractured specimen, long and sparse cracks dominated and this crack was bifurcated at the glass fiber surface.

Acknowlegement

Authors with to thank Mr. Tae Suk Hahm and Kyung Lim Choi for helping tensile and impact experiments.

References

1. J. P. JOG and V. M. NADKARNI (1985) J. Appl. Polym. Sci. 30 : 997
2. J. M. MARGOLIS (1985) Engineering Thermoplastics, Marcel Dekker, New York
3. V.L. SHINGANKULI, J. P. JOG and V. M. NADKARNI (1988) J. Appl. Polym. Sci. 36 : 335
4. G. P. DESIO and L. REBENFELD (1990) J. Appl. Polym. Sci. 39 : 825
5. D. R. BUDGELL and M. DAY(1991) Polym. Eng, Sci. 31 : 1271
6. J. M. KENNY and A. MAFFEZZOLI (1991) Polym. Eng. Sci. 31 : 607
7. L. REBENFELD, G. P. DESIO and J. C. WU (1991)J. Appl. Polym. Sci. 42 : 801
8. J. D. MENCZEL and G. L. COLLINS (1992) Polym. Eng. Sci. 32 : 1264
9. J. S. CHUNG and P. CEBE (1992) Polymer 33 : 2312
10. G. P. DESIO and L. REBENFELD (1992) J. Appl. Polym. Sci. 44 : 1989
11. N. A. MEHL and L. REBENFELD (1992) Polym. Eng. Sci. 32 : 1451
12. K. MAI, M. ZHANG, H. ZENG and S. QI (1994) J. Appl. Polym. Sci. 51 : 57
13. C. AUER, G. KALINKA, TH. KRAUSE and G. HINRICHSEN (1994) J. Appl. Polym. Sci. 51 : 407
14. D. R. FAGERBURG, J. J. WATKINS and P. B. LAWRENCE (1993) J. Appl. Polym. Sci. 50 : 1903
15. L. CARAMARO, B. CHABERT, J. CHAUCHARD and T. VU-KHANH (1991) Polym. Eng. Sci. 31: 1279
16. J. S. CHUNG and P. CEBE (1992) Polymer 33 : 1594
17. M. T. HEINO and J. V. SEPPALA (1992) J. Appl. Polym. Sci. 44 : 2185